



HHS Public Access

Author manuscript

Cancer Gene Ther. Author manuscript; available in PMC 2013 June 01.

Published in final edited form as:

Cancer Gene Ther. 2012 December ; 19(12): 839–844. doi:10.1038/cgt.2012.68.

A Steep Radioiodine Dose Response Scalable to Humans in Sodium Iodide Symporter (NIS) Mediated Radiovirotherapy for Prostate Cancer

Miguel A. Trujillo¹, Michael J. Oneal², Samantha McDonough¹, Rui Qin³, and John C. Morris^{1,4}

¹Department of Internal Medicine, Division of Endocrinology, Diabetes, Metabolism, Nutrition, Mayo Clinic, Rochester, MN

²Department of Molecular Medicine, Mayo Clinic, Rochester, MN Rochester, Minnesota 55905

³Department of Health Sciences Research, Mayo Clinic, Rochester, MN

Abstract

The sodium iodide symporter (NIS) directs the uptake and concentration of iodide in thyroid cells. We have extended the use of NIS-mediated radioiodine therapy to prostate cancer. We have developed a prostate tumor specific conditionally replicating adenovirus (CRAd) that expresses hNIS (Ad5PB_RSV-NIS). For radiovirotherapy to be effective in humans, the radioiodine dose administered in the pre-clinical animal model should scale to the range of acceptable doses in humans. We performed ¹³¹I dose-response experiments aiming to determine the dose required in mice to achieve efficient radiovirotherapy. Efficacy was determined by measuring tumor growth and survival times. We observed that individual tumors display disparate growth rates which preclude averaging within a treatment modality indicating heterogeneity of growth rate. We further show that a statistic and stochastic approach must be used when comparing the effect of an anti-cancer therapy on a cohort of tumors. Radiovirotherapy improves therapeutic value over virotherapy alone by slowing the rate of tumor growth in a more substantial manner leading to an increase in survival time. We also show that the radioiodine doses needed to achieve this increase scaled well within the current doses used for treatment of thyroid cancer in humans.

Keywords

prostate cancer; probasin; adenovirus; sodium iodide symporter; virotherapy; gene therapy; allometry

Users may view, print, copy, download and text and data- mine the content in such documents, for the purposes of academic research, subject always to the full Conditions of use: http://www.nature.com/authors/editorial_policies/license.html#terms

⁴Address Correspondence to: John C. Morris III ¹ Department of Internal Medicine, Division of Endocrinology, Diabetes, Metabolism, Nutrition, Mayo Clinic, Rochester 200 First Street SW Rochester, MN 55905, Telephone: 284-3844/284-9655, morris.john@mayo.edu.

AUTHOR DISCLOSURE STATEMENT

No competing financial interests exist

Introduction

Prostate cancer is the second leading cause of cancer death in men ¹. To date, no uniformly curative therapy for metastatic prostate cancer has been developed. In some malignancies, for which existing treatment regimens are not completely effective, suicide gene therapy and virotherapy strategies targeting the tumor-associated genetic alterations represent rational directions for the development of novel therapeutics ²⁻⁴.

The sodium iodide symporter (NIS) is a transmembrane glycoprotein that mediates uptake of iodide into cells, especially thyroid follicular cells ^{5, 6}. The presence of NIS on the basolateral membrane of thyroid cells has been exploited for many years for diagnostic imaging purposes as well as for ablative therapy of differentiated thyroid cancer using radioactive iodide (¹³¹I). This non-invasive therapy has proven to be a safe and effective treatment for thyroid cancer, even in advanced, metastatic disease ^{7, 8}. In order to extend the use of NIS-mediated radioiodine therapy to other types of cancer, we have successfully transferred and expressed the sodium-iodide symporter (NIS) gene in prostate, colon, and breast cancer cells, both *in vivo* and *in vitro*, using adenoviral vectors. Our experience with adenovirus-mediated NIS transfer and radioiodine therapy was confirmed in large animal model and has culminated in the opening of a phase I trial for prostate cancer that is currently accruing patients ⁹⁻¹³.

Two major problems need to be circumvented to translate gene therapy into the clinical setting. First the limited ability to efficiently transduce tumors with effective levels of therapeutic transgenes has been identified as the fundamental barrier to effective cancer gene therapy ^{14, 15}. A second conclusion that can be drawn from recent virotherapy clinical trials is that multimodal therapy, combining virotherapy (i.e. viral mediated tumor cytolysis) with chemo- or radiotherapy may be necessary for more complete tumor eradication as opposed to mono-therapy using virotherapy alone ¹⁶.

Our approach towards the current problems associated with virotherapy/gene therapy has been the development of tumor specific, conditionally replicating adenoviral vectors that also harbor the NIS gene ¹⁷. In this conditionally replicating adenovirus (CRAd) Ad5PB_RSV-NIS, the transcriptional control of the E1A gene is governed by a composite probasin promoter to reduce extratumoral toxicity and induce tumor selective replication and tumor lysis. NIS expression allows for non-invasive imaging as well as radioiodine mediated therapy. This combination of virus mediated oncolysis and NIS mediated radioiodine therapy has been termed "Radiovirotherapy" ¹⁸. However, for radiovirotherapy to be effective in humans, the radioiodine dose administered to the pre-clinical animal must scale to the range of acceptable doses in humans. Despite the fact that the principles of allometric scaling were put forward as far as back as 1936, they are still poorly understood ^{19, 20}. These principles are based upon the observation that the overall metabolic rate decreases as animals get larger. Thus, calculating equivalent doses from smaller to larger animals (or humans) using linear extrapolation based solely on weight leads to overdosing that can lead to unreasonable doses and even disastrous consequences ²¹⁻²³. Thus, allometric scaling of human acceptable range of doses should be tested on pre-clinical animals to ascertain their efficacy.

An effort to characterize the objective response to anti-cancer treatments culminated with the adoption of the response evaluation criteria in solid tumors (RECIST) guidelines by the World Health Organization ²⁴. Tumor growth has been one of the metrics used to determine the effect of anti-cancer treatments and a number of methods of modeling tumor growth have been developed. In particular for radiovirotherapy, these tumor growth models are based on analytical functions of population dynamics and assume the existence of equilibrium points related to the outcome of the therapy ²⁵. However, these models also assume that, within a cohort, tumor growth is homogenous. Experience shows that this is not the case, since, for most tumor growth curves found in the literature, large standard deviations have been observed.

Using the Ad5PB_RSV-NIS CRAAd, we report here a ¹³¹I dose-response study with the aim to determine the dose required in mice to achieve efficient radiovirotherapy. Our findings show that these doses can be fully scaled to the doses used in humans for treatment of thyroid cancer.

Materials and Methods

CRAAd Construction

The structure Ad5PB_RSV-NIS CRAAd was described elsewhere ¹⁷.

Cell Culture

The Androgen-dependent (LnCaP), prostate cancer cell line was cultured as described ¹².

Animal Experiments

Experimental protocols were approved by and experiments were completed under the guidelines of the Mayo Foundation Institutional Animal Care and Use Committee. All animals were purchased from Harlan Laboratories (Indianapolis, IN) and maintained in the Mayo Foundation animal barrier facilities.

Subcutaneous Tumor Model

Xenografts derived from the LnCaP cell line were established into the right flanks of 4–6-week-old athymic nude Foxn1nu mice (Harlan) by subcutaneous injection of 4×10^6 cells resuspended in 0.125 ml media and 0.125 ml of BD Matrigel basement membrane matrix (BD Biosciences, Bedford, MA). Mice were maintained on a low iodine diet and T4 supplementation (5mg/l) in their drinking water throughout the duration of the experimentation to maximize radioisotope uptake in the tumor and minimize uptake by the thyroid. The mice were examined daily for tumor development.

Efficacy Studies

All mice were subcutaneously engrafted with LnCaP as described above. Mice were divided into groups (average group size $n=10\pm 3$) randomly at time 0. The average tumor size at time 0 was 125 ± 30 mm³. One group of mice was used as control (C), a second group received a single intratumoral dose of Ad5PB_RSV-NIS at 10^{11} vp diluted in PBS in a total volume of 100 μ l (virotherapy V), and the following groups received a single intratumoral injection of

Ad5PB_RSV-NIS at 10^{11} vp and 4 days later a single intraperitoneal dose of ^{131}I of 0.5, 1, 2, or 3 mCi (18.5, 37, 74, and 111 MBq respectively). Tumor volume was measured twice weekly and mice were sacrificed as they met euthanization criteria established by Mayo Foundation Institutional Animal Care and Use Committee.

Results

Radioiodine dose-response; Tumor Growth

One key question about the feasibility of radiovirotherapy is whether the minimal effective radioiodine dose that is required for efficacy in animal models can be translated to humans. To answer this question, LnCap xenografts were established in four groups of mice (average group size $n=10\pm 3$). One group of mice was used as control (C), a second group received a single intratumoral dose of Ad5PB_RSV-NIS at 10^{11} vp (virotherapy V), and the following groups received a single intratumoral injection of Ad5PB_RSV-NIS at 10^{11} vp and 4 days later a single intraperitoneal dose of, 0.5, 1, or 3 mCi ^{131}I . Scaling from a 0.02 kg mouse to a 75 kg humans these doses will be equivalent to 4.6GBq (124 mCi), 9.2 GBq (248 mCi), and 27.5 GBq (744 mCi) respectively using the Body Surface Area (BSA) method ²⁶. Tumor volume was measured twice weekly for a total of 21 days. Tumor growth curves were constructed (Figure 1) and analyzed following three models: Linear, logistic, and Gompertz ²⁵ and the best fit was determined (Table I). In the linear model, all slopes were different from 0 except for mice treated with virus plus 3 mCi of ^{131}I . Fitting the growth curves by the logistic model yielded the same result, in that only in mice treated with virus plus 3 mCi the model did not converge. We then used the more stringent Gompertz model. In this model, mice treated with virus plus 1 or 3 mCi of the ^{131}I radioisotope could not be modeled. These results indicate that, despite the fact that tumor growth is slowed by virotherapy, tumors continue to grow. On the other hand, the fact that tumor growth could not be fitted by either a logistic or a Gompertz model in the radiovirotherapy cohorts when doses of 1 or 3 mCi of the ^{131}I were administered indicates that radiovirotherapy induced a profound negative effect on tumor growth. This observation is in agreement with a previous report in which more sophisticated fitting equations which take into account the dynamic states between the combined effects of tumor growth, virus replication, and radiation are needed to fit tumor growth following radiovirotherapy ²⁵. Taking together, our data indicates that a minimal dose of 1 mCi of therapeutic radioiodine is necessary for radiovirotherapy to improve on virotherapy alone.

Although modeling tumor growth using analytical functions yields useful information, the large standard errors (STE) reflect wide intra-group variations in tumor growth. In consequence tumors cannot be averaged within a treatment modality because averaging presumes homogeneity of growth rate. This is demonstrated in figure 2 where the growth of individual tumors within each experimental cohort is graphed. Tumors appear to group in classes with different growth rates even within a single treatment. Therefore, we employed a stochastic approach, rather than an analytical approach, to analyze the effect of virotherapy and radiovirotherapy on tumor outcome. We utilize this test to compare all tumor growth curves shown in figure 2. First the test was applied solely to the control cohort (Figure 2, Controls). The test showed that three distinct and statistically different groups emerge. The

growth curves within each group were averaged to yield a representative curve for the group (Figure 3A). All three groups differed significantly from one another ($p < 0.05$). This analysis confirms that the rate of tumor growth is heterogeneous with an order of growth rate $CG1 > CG2 > CG3$.

We then decided to compare all tumors individually regardless of the treatment received using repeated measures analysis. Since in our first analysis we found that a dose of 0.5 mCi of ^{131}I did not yield any improvement over virus alone, we substituted this dose for a dose of 2 mCi (equivalent to 18.5 GBq (496 mCi) in a 75 kg human). Applying repeated measures analysis, all tumors can be sorted into four statistically significantly different groups according to their growth rate: F, MF, MS, and S (Figure 3B). These four groups range from fast growing tumors (F) to tumors with an apparent zero growth rate (S) in the order $F > MF > MS > S$. The growth rate is independent of tumor size at time 0 since a Kruskal-Wallis One Way Analysis of Variance on Ranks comparing all tumors according to the treatment they were submitted yielded no statistically significant difference ($H = 6.844$ with 4 degrees of freedom. ($P = 0.144$)). Thus the differences in tumor growth rates are intrinsic to each tumor, and not related to its volume at time 0. We then assigned each tumor to its growth rate class. The results in table II indicate treatment causes a shift towards higher numbers of the slower growing tumors. In untreated controls more than half the tumors fell into the fast growing class of tumors (7/12 in group F), while no tumor was scored in the zero growth class (0/12 in group S). The number of tumors in the F group declined abruptly in the virotherapy treatment (2/10 in group S). However, virotherapy alone did not result in shifting of tumors towards the zero growth class (0/10 in group S). On the other hand, treatment with ^{131}I resulted in a significant shift from the fast growing tumors to the more slow growing tumors, including a larger proportion in the zero growth class. This trend was observed with radioiodine dose of 1 mCi and did not vary to a great extent as the radioiodine doses were increased.

Taken together our data indicate that both virotherapy and radiovirotherapy induced an overall decrease the growth rate of the tumors but the combination of radiotherapy and cytolytic virotherapy was superior to virotherapy alone, which was itself a moderate improvement over control. However, this effect was not absolute and different tumors responded differently to the treatment.

Radioiodine dose-response; Survival

Analysis of tumor growth could not be extended past day 21 because, by week 3, a significant number of control animals reached euthanization criteria thus rendering the statistical test meaningless. For a long term study we investigated how treatment with Ad5PB_RSV-NIS CRAAd, with or without ^{131}I radiotherapy, impinges on survival. The survival times of each group were graphed using Kaplan-Meier curves (Figure 4). The end point event was set at tumor burden $1,000 \text{ mm}^3$, while death before end point was considered as censoring. By week 8 all animals in the control group reached tumor sizes $1,000 \text{ mm}^3$ and, according our animal use committee guidelines, were euthanized. Virotherapy resulted in a net improvement in survival over the control group. Thus, while all control animals have died by week 8, members of the virotherapy group survived up to week

10. Treatment with ^{131}I greatly improved the probability of survival beyond that achieved with virotherapy alone. The survival times were subjected to a Cox proportional hazards survival regression model (Figure 4). The hazard ratio of virotherapy vs. control was 0.342 ($p=0.024$) while radiovirotherapy yielded hazard ratio compared to control ranging from 0.29 to as low as 0.15 and p values that were between one and two order of magnitude lower than those of virotherapy alone. Again, treatment with 1 mCi ^{131}I was sufficient to improve the treatment result, but escalating the dose up to 3 mCi did not significantly improve the efficacy (Figure 4). These results confirm that the combination of radiotherapy and cytolytic virotherapy was superior to virotherapy alone.

Correlation tumor growth to survival time

Because we followed rate the of tumor growth and survival time in individual mice, we can compare and correlate these two parameters. We scored the frequency of animal death at a particular time and compared that with the frequency of the growth classes of tumor. It can be clearly seen in figure 5 that mice bearing fast growing tumors F died within the first 5 weeks while mice bearing more slowing growing tumors reached the censoring size later in time. By week 13, of the 7 mice that were still alive, 6 bore tumors of type S and one of type MF. Of these, 3 were treated with virus plus 1 mCi ^{131}I and 4 with 3 mCi. Thus, a strong correlation between the rate of tumor growth and the survival time was found thus validating the growth analysis. Moreover, this result also shows that only mice treated with radiovirotherapy have a better probability of survival. Finally, these results also reinforce the finding that 1 mCi of ^{131}I was sufficient for the improvement of radiovirotherapy over virotherapy alone. Increasing the dose to 3 mCi did not result in a significant increase of efficacy when compared to lower doses.

Discussion

We have reported the use of prostate targeted conditionally replicating adenoviruses expressing the NIS protein in *in vivo* mouse models of prostate cancer¹⁷. We have shown in this report that a dose of 1 mCi of ^{131}I is sufficient to provoke a tumor response that is superior to that of virotherapy alone. Hence, a steep dose response to ^{131}I treatment in which a jump from no effect at 0.5 mCi to full effect at 1 mCi was observed. Moreover, a plateau was reached at 1 mCi since increasing the dose to 2 and 3 mCi did not produce any additional benefit. This observation suggests that a saturation in the NIS ability to pump and concentrate circulating radioiodine into the tumor is reached at a dose of 1 mCi.

The idea of the use of the NIS gene as a therapeutic gene for malignant diseases arose from the utility and efficacy of ^{131}I therapy in thyroid cancer patients⁸. One of the central questions in the translation of this NIS-based methodology into the clinic is whether the doses of radioiodine used in the animal models are scalable to humans. Dose conversions have by some authors been based on linear extrapolation based solely on weight. Based on their calculations, Siddiqui et al. found that the $\text{Na}^{99\text{m}}\text{TcO}_4$ dose needed for NIS-mediated imaging in dogs was ten times larger than that to be administered to humans, when in fact the human equivalent dose (HED) if calculated based on BSA and their experimental observations is only two times larger²⁷. Two major methods have been used to plan

radioiodine dosing in humans: empiric fixed doses, and dosimetrically determined doses. While the most common empirical ^{131}I doses for advanced thyroid cancer range from 150 mCi to 300 mCi, dosimetrically determined doses can be considerably higher, ranging from 300 mCi to 600 mCi²⁸. The Food and Drug Administration of the United States (FDA) formulated a table of dose conversion factors that allow for allometric adaptation from pre-clinical animals to humans based on body surface area (BSA)²⁹. This table is formulated for 60 kg humans. After adjusting the general BSA formula to for a more realistic 75 kg human²⁶, doses between 1 and 2 mCi of ^{131}I in mice scale to between 248 mCi, and 496 mCi in humans. It has been stressed that using BSA for dose calculation is not fully accurate leading to approximately 10% of patients being overdosed and 30% underdosed. This observation led to the recommendation that BSA should be used to estimate a dose range rather than determining an absolute dose³⁰. Despite these general caveats, the ^{131}I doses that we have used in the current studies in mice fell well within comparable ranges used in humans for treatment of metastatic thyroid cancer.

Measuring tumor growth and the effects that anticancer treatment has on growth rates is a well know measure of the efficacy of the treatment^{25, 31, 32}. Here we show that while analytical functions are useful to model single tumors, this is not the case when dealing with a population of tumors that have or have not received a particular anti-cancer treatment when the response to treatment is highly variable. Individual tumors have disparate growth rates which preclude averaging within a treatment modality because averaging presumes homogeneity of growth rate. We have shown that a statistic and stochastic approach must be used when comparing the effect of an anti-cancer therapy on a cohort of tumors. The growth rate difference is not due to the initial conditions but rather is an intrinsic characteristic of the tumor. This may be due to substantial genetic or epigenetic differences within the cancer stem cells that give rise to the tumor as well as tumor recipient variability³³ and other variable factors regarding delivery or clearing of the therapeutic moiety from the tumor and animal. CD44⁺ prostate cancer cells have been shown to have the stem-like properties of increased tumorigenic, clonogenic, and metastatic potential. However, it was demonstrated previously that the CD44⁺ prostate cells were a heterogenous population containing both primitive stem cells as well as later progenitor cells³⁴. Hurt et al. later identified a rare subpopulation of CD44⁺CD24⁻ prostate cancer cells with stem-like characteristics such as increased clonogenic and tumorigenic properties, and the ability to grow as nonadherent spheres in serum-replacement medium³⁵. However, this subpopulation of cells represent only 0.04% of the total LNCaP cells in culture and, tumors from mice injected with CD44⁺CD24⁻ cells phenotypically resembled tumors removed from mice injected with total LNCaP cells. This indicates that CD44⁺CD24⁻ cells can give rise to the heterogeneous population present in tumors derived from the LNCaP cell line. Thus, tumor heterogeneity is an intrinsic property probably dictated by the nature of the stem cell population of the tumor. Contrary to a previous report³⁶, we have found that the initial conditions (e.g. tumor volume at time 0) is not a factor influencing the outcome of the treatment in our model. In fact, in the current studies, the tumor volumes at time 0 were not significantly different, yet the rates of tumor growth varied highly within a particular treatment modality group, also including the control group that received no therapy at all. Nonetheless, the results show that virotherapy treatment shifted the distribution of tumors from fast growing towards more

slowing growing tumors. This shift was enhanced by radiovirotherapy. Shifting the growth rate to slower growing tumors resulted in an increase in the survival time as indicated by the strong correlation between survival probability and rate of tumor growth. It is interesting that these observations recapitulate the variable response to treatment of cancer in many human models as described by RECIST guidelines²⁴ despite the use of cloned cell lines in our animal based experiments. Thus, the tumor response to anti-cancer treatments appears as a stochastic response not deterministic. The fact that both *in vitro* and *in vivo* proliferating cancer cells divide asymmetrically to produce progeny cells with different proliferating rates may explain that the rates of tumor growth are not homogeneous in the untreated control tumor as well as the stochastic nature of treatment outcome³⁷.

In conclusion we show here that radiovirotherapy improves therapeutic value over virotherapy alone by slowing the rate of tumor growth and improving survival time. We also show that the radioiodine doses needed to achieve this increase scaled well within the current doses used for treatment of thyroid cancer in humans.

Acknowledgments

The authors wish to thank Tracy Decklever at the Nuclear Medicine Animal Imaging Resource Mayo Clinic, Rochester for technical help and Dr. David Dingli at the Department of Molecular Medicine, Mayo Clinic, Rochester MN for helpful discussion. This work was supported by Prostate SPOR grant P50 CA 091956, Donald J. Tindall, P.I., John C. Morris, Project Director.

References

1. Ruijter E, van de Kaa C, Miller G, Ruiter D, Debruyne F, Schalken J. Molecular genetics and epidemiology of prostate carcinoma. *Endocr Rev.* 1999; 20(1):22–45. [PubMed: 10047972]
2. Chiocca EA, Broaddus WC, Gillies GT, Visted T, Lamfers ML. Neurosurgical delivery of chemotherapeutics, targeted toxins, genetic and viral therapies in neuro-oncology. *J Neurooncol.* 2004; 69(1–3):101–17. [PubMed: 15527083]
3. McCormick F. Cancer gene therapy: fringe or cutting edge? *Nat Rev Cancer.* 2001; 1(2):130–41. [PubMed: 11905804]
4. Yamamoto M, Curiel DT. Cancer gene therapy. *Technol Cancer Res Treat.* 2005; 4(4):315–30. [PubMed: 16029053]
5. Carrasco N. Iodide transport in the thyroid gland. *Biochim Biophys Acta.* 1993; 1154(1):65–82. [PubMed: 8507647]
6. Jhiang SM, Cho JY, Ryu KY, DeYoung BR, Smanik PA, McGaughy VR, et al. An immunohistochemical study of Na⁺/I⁻ symporter in human thyroid tissues and salivary gland tissues. *Endocrinology.* 1998; 139(10):4416–9. [PubMed: 9751526]
7. Van Nostrand D, Wartofsky L. Radioiodine in the treatment of thyroid cancer. *Endocrinol Metab Clin North Am.* 2007; 36(3):807–22. vii–viii. [PubMed: 17673129]
8. ELM. Carcinoma of follicular epithelium: Radioiodine and other treatments and outcomes. In: Braverman, LE.; Utiger, RD., editors. *The Thyroid: A Fundamental and Clinical Text.* 7. Lippincott - Raven; Philadelphia: 1996. p. 922–945.
9. Scholz IV, Cengic N, Baker CH, Harrington KJ, Maletz K, Bergert ER, et al. Radioiodine therapy of colon cancer following tissue-specific sodium iodide symporter gene transfer. *Gene Therapy.* 2005; 12(3):272–80. [PubMed: 15510175]
10. Dwyer RM, Schatz SM, Bergert ER, Myers RM, Harvey ME, Classic KL, et al. A preclinical large animal model of adenovirus-mediated expression of the sodium-iodide symporter for radioiodide imaging and therapy of locally recurrent prostate cancer. *Mol Ther.* 2005; 12(5):835–41. [PubMed: 16054438]

11. Dwyer RM, Bergert ER, O'Connor MK, Gendler SJ, Morris JC. Sodium Iodide symporter-mediated radioiodide imaging and therapy of ovarian tumor xenografts in mice. *Gene Ther.* 2006; 13:60–66. [PubMed: 16121204]
12. Spitzweg C, Dietz AB, O'Connor MK, Bergert ER, Tindall DJ, Young CY, et al. In vivo sodium iodide symporter gene therapy of prostate cancer. *Gene Therapy.* 2001; 8(20):1524–31. [PubMed: 11704812]
13. Morris, JC. 2009. <http://clinicaltrials.gov/ct/show/NCT00788307>
14. Herrmann F. Cancer gene therapy: principles, problems, and perspectives. *J Mol Med.* 1995; 73(4): 157–63. [PubMed: 7627636]
15. Waehler R, Russell SJ, Curiel DT. Engineering targeted viral vectors for gene therapy. *Nat Rev Genet.* 2007; 8(8):573–87. [PubMed: 17607305]
16. Chu RL, Post DE, Khuri FR, Van Meir EG. Use of replicating oncolytic adenoviruses in combination therapy for cancer. *Clin Cancer Res.* 2004; 10(16):5299–312. [PubMed: 15328165]
17. Trujillo MA, Oneal MJ, McDonough S, Qin R, Morris JC. A probasin promoter, conditionally replicating adenovirus that expresses the sodium iodide symporter (NIS) for radiovirotherapy of prostate cancer. *Gene Therapy.* 2010; 17(11):1325–1332. [PubMed: 20428214]
18. Dingli D, Peng KW, Harvey ME, Greipp PR, O'Connor MK, Cattaneo R, et al. Image-guided radiovirotherapy for multiple myeloma using a recombinant measles virus expressing the thyroidal sodium iodide symporter. *Blood.* 2004; 103(5):1641–6. [PubMed: 14604966]
19. Du Bois, EF. *Basal Metabolism in Health and Disease.* Lea and Febiger; Philadelphia, Pennsylvania, USA: 1936.
20. Sharma V, McNeill JH. To scale or not to scale: the principles of dose extrapolation. *Br J Pharmacol.* 2009; 157(6):907–21. [PubMed: 19508398]
21. West LJ, Pierce CM, Thomas WD. Lysergic Acid Diethylamide: Its Effects on a Male Asiatic Elephant. *Science.* 1962; 138(3545):1100–3. [PubMed: 17772968]
22. A compound in red wine makes mice live longer, healthier. *Mayo Clin Health Lett.* 2007; 25(5):4.
23. Baur JA, Pearson KJ, Price NL, Jamieson HA, Lerin C, Kalra A, et al. Resveratrol improves health and survival of mice on a high-calorie diet. *Nature.* 2006; 444(7117):337–42. [PubMed: 17086191]
24. Therasse P, Arbuck SG, Eisenhauer EA, Wanders J, Kaplan RS, Rubinstein L, et al. New guidelines to evaluate the response to treatment in solid tumors. European Organization for Research and Treatment of Cancer, National Cancer Institute of the United States, National Cancer Institute of Canada. *J Natl Cancer Inst.* 2000; 92 (3):205–16. [PubMed: 10655437]
25. Dingli D, Cascino MD, Josic K, Russell SJ, Bajzer Z. Mathematical modeling of cancer radiovirotherapy. *Math Biosci.* 2006; 199(1):55–78. [PubMed: 16376950]
26. Reagan-Shaw S, Nihal M, Ahmad N. Dose translation from animal to human studies revisited. *Faseb J.* 2008; 22(3):659–61. [PubMed: 17942826]
27. Siddiqui F, Barton KN, Stricker HJ, Steyn PF, Larue SM, Karvelis KC, et al. Design considerations for incorporating sodium iodide symporter reporter gene imaging into prostate cancer gene therapy trials. *Hum Gene Ther.* 2007; 18(4):312–22. [PubMed: 17408358]
28. Van Nostrand D, Atkins F, Yeganeh F, Acio E, Bursaw R, Wartofsky L. Dosimetrically determined doses of radioiodine for the treatment of metastatic thyroid carcinoma. *Thyroid.* 2002; 12(2):121–34. [PubMed: 11916281]
29. USFDA. *Guidance for Industry: Estimating the Maximum Safe Starting Dose in Adult Healthy Volunteer.* US Food and Drug Administration; Rockville, MD: 2005.
30. Gurney H. How to calculate the dose of chemotherapy. *Br J Cancer.* 2002; 86(8):1297–302. [PubMed: 11953888]
31. Kozusko F, Bourdeau M, Bajzer Z, Dingli D. A microenvironment based model of antimetabolic therapy of Gompertzian tumor growth. *Bull Math Biol.* 2007; 69(5):1691–708. [PubMed: 17577604]
32. Bajzer Z, Carr T, Josic K, Russell SJ, Dingli D. Modeling of cancer virotherapy with recombinant measles viruses. *J Theor Biol.* 2008; 252(1):109–22. [PubMed: 18316099]

33. Rosen JM, Jordan CT. The increasing complexity of the cancer stem cell paradigm. *Science*. 2009; 324(5935):1670–3. [PubMed: 19556499]
34. Patrawala L, Calhoun T, Schneider-Broussard R, Li H, Bhatia B, Tang S, et al. Highly purified CD44+ prostate cancer cells from xenograft human tumors are enriched in tumorigenic and metastatic progenitor cells. *Oncogene*. 2006; 25(12):1696–708. [PubMed: 16449977]
35. Hurt EM, Kawasaki BT, Klarmann GJ, Thomas SB, Farrar WL. CD44+ CD24(-) prostate cells are early cancer progenitor/stem cells that provide a model for patients with poor prognosis. *Br J Cancer*. 2008; 98(4):756–65. [PubMed: 18268494]
36. Rommelfanger DM, Offord CP, Dev J, Bajzer Z, Vile RG, Dingli D. Dynamics of melanoma tumor therapy with vesicular stomatitis virus: explaining the variability in outcomes using mathematical modeling. *Gene Ther*. 2011
37. Dey-Guha I, Wolfer A, Yeh AC, Albeck GJ, Darp R, Leon E, et al. Asymmetric cancer cell division regulated by AKT. *Proc Natl Acad Sci U S A*. 2011; 108(31):12845–50. [PubMed: 21757645]

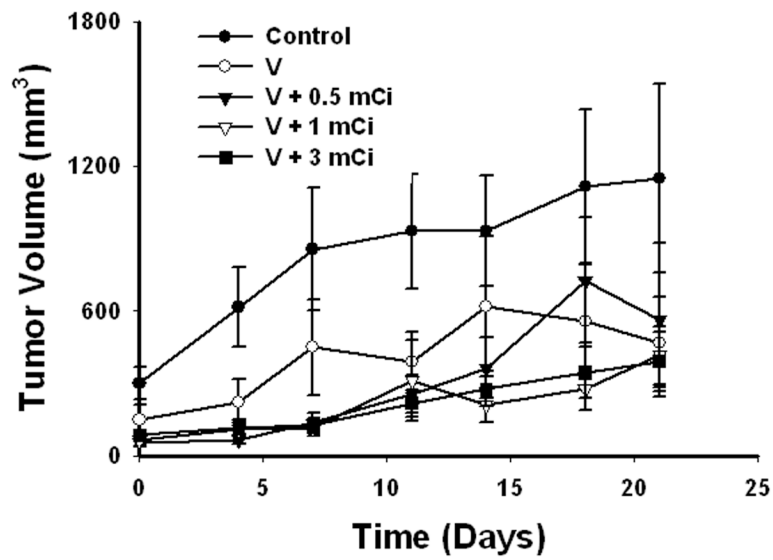


FIGURE 1. Tumor growth kinetics

Mice were subcutaneously engrafted with LnCaP, one group of mice was used as control (C), a second group received a unique intratumoral dose of Ad5PB_RSV-NIS at 10^{11} vp (virotherapy V), and the remaining groups received a unique intratumoral dose of Ad5PB_RSV-NIS at 10^{11} vp and 4 days later a single ^{131}I intraperitoneal dose of 0.5, 1, or 3mCi. The average group size is $n=10 \pm 3$.

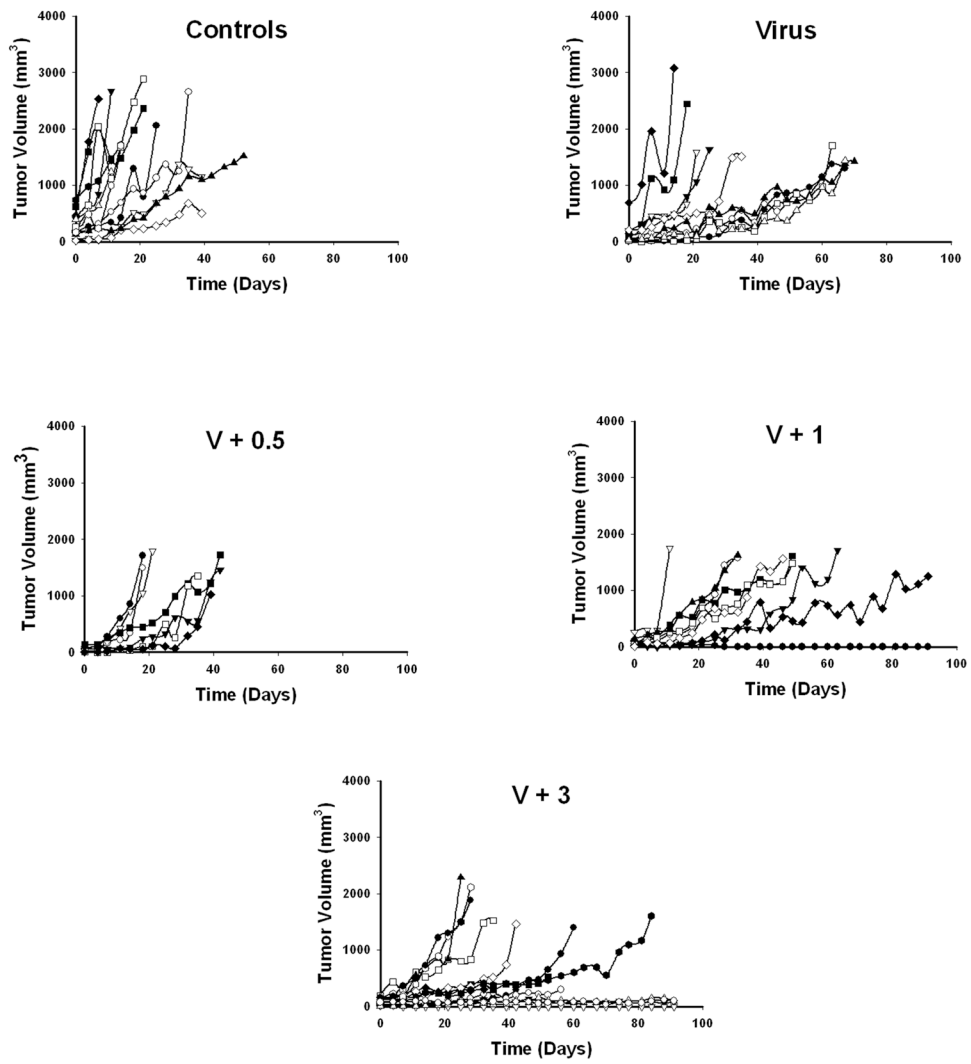
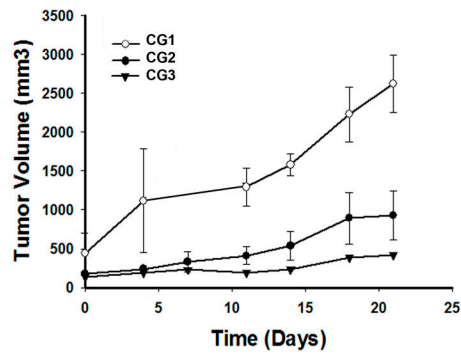
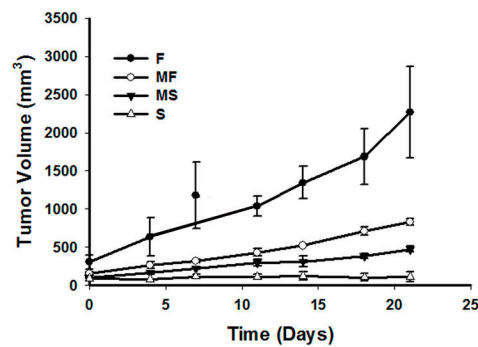
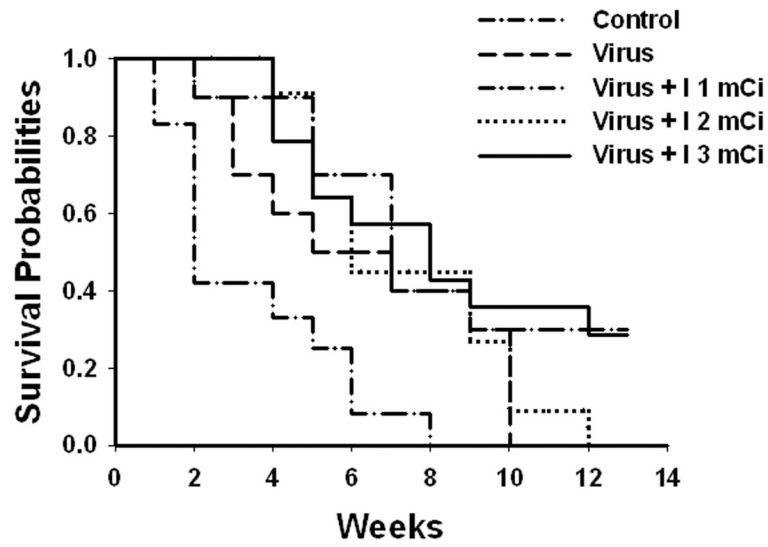


FIGURE 2. Tumor growth kinetics

The individual growth curves for each tumor within a treatment modality are shown.

A**B****FIGURE 3. Repeated measures analysis**

A) The tumor growth of the individual tumors within the control cohort was analyzed using the repeated measures test. Three statistically significantly different groups of tumors, termed CG1, CG2, and CG3, were revealed in which each group differs by its rate of growth. B) The same test was applied to all tumors regardless of the treatment. Here four different groups of tumors, termed F, MF, MS, and S were revealed in which each group differs by its rate of growth.



	Risk	Lo95%	Hi95%	p	pChi
Control	-	-	-	-	0.0035
V	0.34227	0.1349	0.8709	0.0244	
V+1	0.1829	0.0674	0.4961	0.0008	
V+2	0.2853	0.1184	0.6877	0.0052	
V+3	0.1488	0.0537	0.4120	0.0002	

FIGURE 4. Survival analysis
 Survival was plotted according to Kaplan-Meier and analyzed using the Cox proportional hazards survival regression.

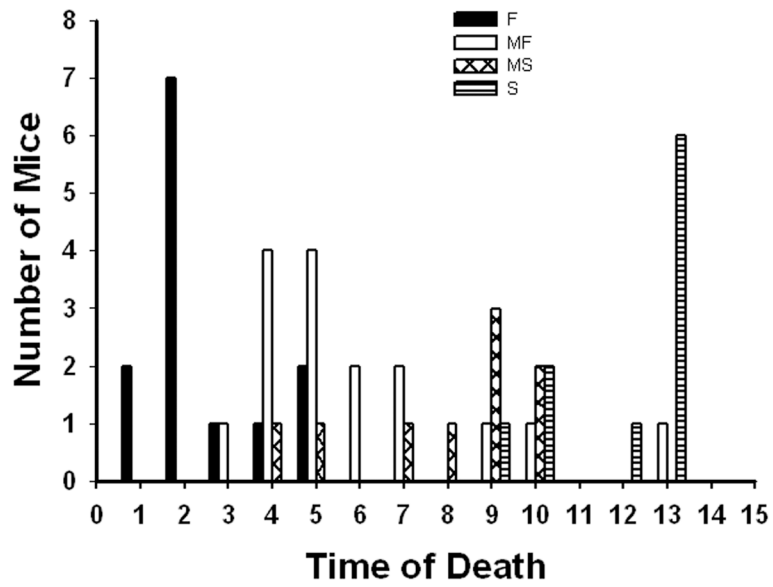


FIGURE 5. Correlation between tumor growth and survival time

The number of mice sacrificed at a particular time was correlated to the classes of tumor, as found in figure 3B, it bore and plotted as a graph bar of time of death vs. number of sacrificed mice for each of the four groups.

Table I

Tumor Growth Curves Models

	Linear (Test: slope = 0)	Logistic	Gompertz
Control	Fit	Fit	Fit
Virus	Fit	Fit	Fit
Virus + 0.5 mCi ¹³¹ I	Fit	Fit	Fit
Virus + 1 mCi ¹³¹ I	Fit	Fit	Does not Fit
Virus + 3 mCi ¹³¹ I	Does not Fit	Does not Fit	Does not Fit

The tumor growth curves were fitted according to a linear, a logistic, or a Gompertz model. p-values were estimated to validate the fitting model. p<0.05 model does not fit, p> 0.05 model fits

Table II

Group Distribution

	F	MF	MS	S	Total
Control	7	4	1	0	12
V	2	4	4	0	10
V+I1	1	5	2	2	10
V+I2	3	4	0	4	11
V+I3	0	3	6	4	13
Total	13	20	13	10	56

Based on the repeated measures test, all tumor growth curves were grouped into its corresponding growth pattern.